

Article

Study on the Mineralogical and Geochemical Characteristics of Arsenic in Permian Coals: Focusing on the Coalfields of Shanxi Formation in Northern China

Liqun Zhang ^{1,2}, Liugen Zheng ^{1,2,*} and Meng Liu ¹

¹ School of Resources and Environmental Engineering, Anhui University, Hefei 230093, China; x21101001@stu.ahu.edu.cn (L.Z.); x19101001@stu.ahu.edu.cn (M.L.)

² Anhui Province Engineering Laboratory for Mine Ecological Remediation, Anhui University, Hefei 230601, China

* Correspondence: lgzheng@ustc.edu.cn; Tel./Fax: +86-551-63861471

Abstract: The Huainan Coalfield is a typical multi-coal seam coalfield. In order to systematically investigate the distribution, occurrence, and integration of arsenic (As) in Shanxi coal, 26 coal samples and three rock samples were collected in the No. 1 coal seam of Huainan coalfield. The minerals, major element oxides, and As were analyzed by X-ray diffraction (XRD), scanning electron microscopy (SEM), polarized light microscopy, X-ray fluorescence spectroscopy (XRF) and inductively coupled plasma-mass spectrometry (ICP-MS). The results indicated that the coals of Shanxi Formation were characterized by very low ash yields and low total sulfur contents. The identified minerals by XRD in the studied coals are dominated by kaolinite, quartz, calcite, and a lesser amount of pyrite. The As content ranges from 10.33 mg/kg to 95.03 mg/kg, with an average of 44.74 mg/kg. Compared with world coals, the studied coals have higher contents of As, which are characterized by enrichment. Based on statistical analyses, As shows an affinity to ash yield and possible association with silicate minerals. The contents of As in all occurrence fractions were ranked from high to low as follows: residual > Fe-Mn oxides > organic > exchangeable > carbonate. Using $B, w(\text{Sr})/w(\text{Ba})$ and $w(\text{B})/w(\text{Ga})$ geochemical parameter results to invert the depositional environment of the Huainan Shanxi Formation, a suitable coal-forming environment can cause relatively enriched As in coal.

Keywords: coalfield; arsenic; enrichment; depositional environment



Citation: Zhang, L.; Zheng, L.; Liu, M. Study on the Mineralogical and Geochemical Characteristics of Arsenic in Permian Coals: Focusing on the Coalfields of Shanxi Formation in Northern China. *Energies* **2022**, *15*, 3185. <https://doi.org/10.3390/en15093185>

Academic Editors: Jing Li, Yidong Cai, Lei Zhao and Rajender Gupta

Received: 11 March 2022

Accepted: 21 April 2022

Published: 27 April 2022

Publisher's Note: MDPI stays neutral with regard to jurisdictional claims in published maps and institutional affiliations.



Copyright: © 2022 by the authors. Licensee MDPI, Basel, Switzerland. This article is an open access article distributed under the terms and conditions of the Creative Commons Attribution (CC BY) license (<https://creativecommons.org/licenses/by/4.0/>).

1. Introduction

China is the world's largest energy consumer, with coal as the main fuel for its energy consumption [1]. Coal contains potentially harmful trace elements, of which As is receiving increasing attention due to its volatility, toxicity, and carcinogenicity [2,3]. As one of the volatile elements in coal, As will be released in the process of coal processing and combustion, which may seriously affect the soil and water quality around the mining area, interfere with the normal function of the immune system, and pose a threat to human health. Therefore, As concentrations and its mode of occurrence in coal have been studied by several researchers during the last three decades [4–7]. These studies show that As enrichments in coal could be controlled by several parameters, such as presence of As-bearing sulfide minerals, clastic influx and/or influence of seawater into paleomires, redox conditions within paleomires, or influence of hydrothermal solutions during coalification.

The previous studies show that Chinese coals display variable ash yields, and some studies reported up to 10 mg/kg As concentrations; however, the As content is significantly different in different coal ages, regions and coal types [8]. In China, high-As coal is widely distributed in point-like distribution, mainly located in the three northeastern provinces of Henan Yima, Shanxi Datong, Guangxi Nanning, Gansu and parts of Yunnan [9]. In addition, the occurrence modes and enrichment origins of As in different regions and different coal

types in China are different. Some scholars have found that the most important geological sources of As in the Santanghu coalfield are related to penetration of fissure-hydrothermal solutions and groundwater into coal seams [10]. It is found that the accumulation of As in the peat mire environment of the Guizhou No. 6, 7, 23, and 27 coal seams is mainly controlled by the marine influence during and/or after peat accumulation [11]. China is rich in coal reserves, and the regions involved in many studies are relatively scattered. Specific to the Huainan Coalfield, previous studies have mainly focused on the Permian Upper Shihezi and Lower Shihezi formations [12–15]. However, with the increase in demand for coal resources, the mining of the Huainan Coalfield has gradually shifted from shallow coal to the deep Shanxi Formation. The influence of As on the environment, and the difficulty and approach to utilize or remove specific trace elements, are mainly dependent on the occurrence of elements [16]. Different occurrence states have a great impact on the migration, transformation, and bioavailability of As in the natural environment. Therefore, it is necessary for us to conduct a systematic study on the As in Shanxi Formation coal.

Some studies have inferred the depositional environment of the Permian coal-bearing strata in the Huainan Coalfield by using the characteristics of geochemistry, mineralogy, paleontology, sedimentary structure, lithology, and coalbeds [17–19]. The Shanxi Formation was an important peat accumulation period in the Huainan Coalfield, and it is distributed in the foreland fold-thrust belt and its frontal area of the Dabie-Sulu orogenic belt. In the early stages of coalification and post-generation rock formation, it experienced multiple stages of strong regional tectonic movements and more frequent seaward-regressive events. A systematic investigation was conducted from the No. 1 seam in the Huainan Coalfield to provide basic data on the characteristics of the coal quality and the geochemical composition. The purpose of this study is to: (1) investigate the chemical characteristics and mineral distribution of Shanxi coal, (2) analyze the occurrence characteristics of As in the coal seam and explore its depositional environment, and (3) discuss the origin of As enrichment. Collectively, the results of this study could provide a theoretical basis for the processing and utilization of associated resources and potential evaluation in the Huainan coalfield.

2. Geological Background

The Huainan coalfield is an important coal production area in east China. It is located in the north-central part of Anhui Province. It extends into the Chuxian area in the east and extends to the vicinity of Fuyang in the west. The coal mining area is 180 km in length, 15–20 km in width and covers an area of 3200 km² (Figure 1). The coal field is a complex syncline structure. The structural features of the main body of the complex syncline in Huainan are distributed in the east-west direction due to the squeezing action of the compressive stress in the north and south. A series of compression-torsional inverse faults, thrust faults and large nappe bodies are developed on the north and south wings of the complex syncline, and the imbricate structure of the two wings of the complex syncline is formed, which makes some strata in the south wing reverse upright.

The Carboniferous-Permian period was an important peat-forming period in the study area [20]. As one of the five major coal fields in China, the Huainan Coalfield is a typical Permian multi-peat forming environment; in turn, up to 21 coal seams are located in the Permian sequences (Figure 2). The coal-bearing strata in the Huainan Coalfield include the Benxi Formation of the Late Carboniferous, the Taiyuan Formation, the Shanxi Formation and the Lower Shihezi Formation of the Early Permian, and the Upper Shihezi Formation of the Late Permian. The Upper Shihezi Formation, the Lower Shihezi Formation, and the Shanxi Formation constitute the main mineable coal-bearing sequences in Huainan, which are a complete deltaic system developed on the offshore bay [2]. Among them, the Shanxi Formation was integrated into the Taiyuan Formation and was in contact with the Lower Shihezi Formation, and the mineable coal seams in this formation are the No. 1 and No. 3 coal seams. The Shanxi Formation shows a set of detrital coal-bearing sequences dominated by deltaic sediments, with a complete cyclonic structure of pre-triangle, delta front, and delta plain deposits. The lower part is a prodelta facies deposit, and its lithology

is mainly siltstone-silty mudstone and dark mudstone. The No. 1 and No. 3 coal seams in the main mineable coal seams are developed in this sedimentary system.

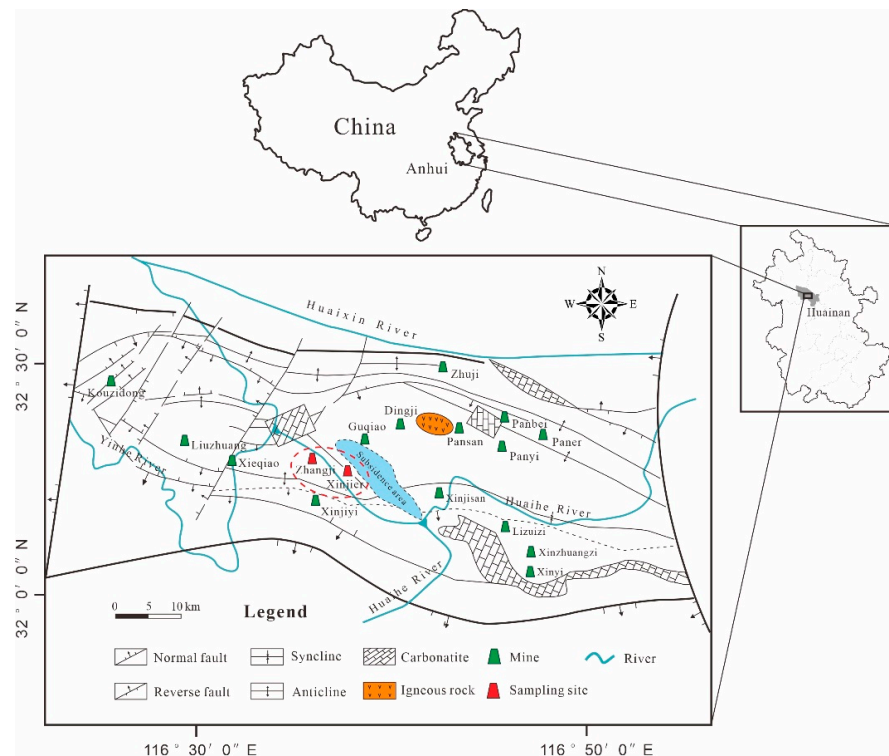


Figure 1. Location map of Huainan Coalfield, China.

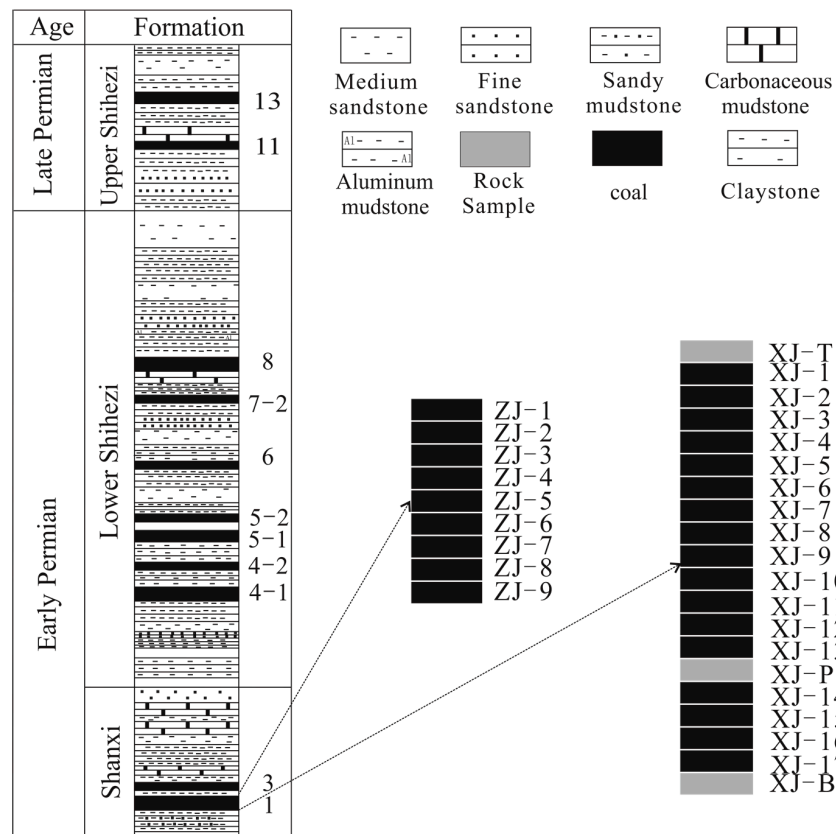


Figure 2. Generalized stratigraphic column and specific sampling points in the study area.

3. Methodology

3.1. Sampling

During the coal exploration studies of the Shanxi Formation coals, a total of twenty-nine samples (including coal, roof, floor, and parting samples) were collected from the Zhangji mine and Xinjier mine by using channel sampling, with a sample taken every 10 cm interval. Among them, the numbers of coal samples are ZJ-1–ZJ-9 and XJ-1–XJ-17, and the roof, the parting, and the floor samples are numbered XJ-T, XJ-P, and XJ-B respectively (Figure 2). All samples were immediately stored in polyethylene bags to prevent contamination, oxidation, and loss of moisture. They were brought back to the laboratory and let dry naturally, then pass through a 200-mesh sieve after grinding.

3.2. Analysis

According to the Chinese National Standard GB/T211-2008, the moisture (M), ash yield (A_d) and volatile matter (V) in coal were measured by automatic industrial analyzer (SDTGA5000a, Sundy, Changsha, China). The sulfate sulfur (S_s), pyritic sulfur (S_p), and organic sulfur (S_o) were determined following GB/T215-2003, and the total sulfur (S_t) was determined following GB/T 214-2007.

Phase-mineral composition of coal was determined by XRD (SmartLab 9, Rigaku Industrial Corporation, Osaka, Japan), acceleration voltage ≤ 45 kV, tube flow ≤ 200 mA, power ≤ 9 kW, scanning range was $2^\circ\sim 160^\circ$ (2θ), 2θ angle indication error was 0.017° , resolution was 27%, and diffraction intensity stability was 1.1%. The fine structure observation was analyzed by SEM (S-4800, Hitachi Corporation, Tokyo, Japan); the secondary electron resolution was 1.0 nm (15 kV), magnification was 20~800, acceleration voltage was 0.1~30 kV, and beam was 1 pA~2 nA. The microscopic morphology of minerals was observed by polarized light microscope (BX53, Olympus, Tokyo, Japan); the microscope condition was manual focusing, the lifting range was 50 mm, and the visual magnification was $40\times\sim 500\times$.

The major oxides were determined by X-ray fluorescence spectrometry (ZSX Primus II type, Rigaku Industrial Corporation, Tokyo, Japan). The 0.1 g sample was accurately weighed in an acidic mixture and digested into a transparent solution on a hot plate at 110°C . Then, each solution was filtered through a $0.45\ \mu\text{m}$ membrane and made up to 25 mL with deionized water with 5% HNO_3 . The trace elements (As, B, Sr, Ba, Ga) in the coal were determined by ICP-MS (Agilent 7500cx, Agilent, Palo Alto, CA, USA). The working parameters of the suppressor were: RF power 1500 W, auxiliary gas (Ar) flow 0.90 L/min, atomizer (Ar) flow 0.25 L/min, and the error analysis was -1.775 ± 2.745 . The interference of ArCl to element As is eliminated by collision cell, and the flow rate of collision gas (He) is 0.7 mL/min. The chemical forms of As were analyzed by a sequential chemical extraction procedure (Table 1), and the recovery was 97.2~101.7%. The accuracy of As was determined by standards reference material GBW11116.

Table 1. Sequential chemical extraction procedure used for arsenic speciation. Adapted with permission from Elsevier, 2022 [2].

Step	Speciation	Extractant	Extraction Conditions	Cellulose Filter
F1	exchangeable	1.00 g sample + 8 mL NaOAc (1 M, pH = 8.2)	oscillate at room temperature of $(25 \pm 2)^\circ\text{C}$ for 1 h, centrifuge	0.1 μm
F2	carbonate	sample recovered in F1 + HOAc (1 M, pH = 5.0)	stir until the reaction is complete at room temperature, then centrifuge	0.1 μm
F3	Fe-Mn oxides	sample recovered in F2 + 20 mL of 0.3 M $\text{Na}_2\text{S}_2\text{O}_4$ + 0.175 M Na-citrate + 0.025 M citrate	occasional stirring at $96 \pm 3^\circ\text{C}$, then centrifuge	0.1 μm
F4	organic	sample recovered in F3 + ① 3 mL of 0.02 M HNO_3 + 5 mL of H_2O_2 (pH = 2); ② 3 mL of 30% H_2O_2 (pH = 2, with HNO_3); ③ 5 mL of 3.2 M NH_4OAc	① 2 h at $85 \pm 2^\circ\text{C}$ ② 3 h at $85 \pm 2^\circ\text{C}$ ③ 0.5 h continuous stirring, then centrifuge	0.1 μm
F5	residual	tailings recovered in F4 + 5 mL HNO_3 + 5 mL HF	digestion at 110°C to clear liquid, and then the cover was lifted at 90°C to remove the acid	0.1 μm

4. Results

4.1. Standard Coal Characteristics

The moisture (M) content of coal in the Zhangji Mine is 1.79~2.17%, with an average of 1.98%. The ash yield (A_d) of coals in the Zhangji Mine is 5.94~13.30%, with an average of 8.38%. The content of volatile matter (V) in Zhangji Mine coal is 29.97~38.04%, with an average of 33.72%. The total sulfur (S_t) content is 0.11~0.37%, with an average of 0.16%, and the pyritic sulfur (S_p), sulfate sulfur (S_s), and organic sulfur (S_o) accounts for 64%, 12%, and 24% of total sulfur, respectively (Table 2).

Table 2. Main coal quality parameter values of coal in the Shanxi Formation in the Huainan Coalfield (%).

Samples	M (%)	A_d (%)	V (%)	S_t (%)	S_p (%)	S_s (%)	S_o (%)
ZJ-1	2.12	5.65	38.04	0.37	0.26	0.02	0.09
ZJ-2	1.79	13.3	29.97	0.20	0.14	0.02	0.04
ZJ-3	2.17	7.44	35.61	0.25	0.17	0.03	0.05
ZJ-4	2.02	6.02	36.43	0.30	0.20	0.05	0.05
ZJ-5	1.81	5.94	33.26	0.22	0.15	0.04	0.03
ZJ-6	2.07	6.03	36.26	0.28	0.18	0.04	0.06
ZJ-7	1.93	11.90	31.60	0.17	0.08	0.02	0.07
ZJ-8	1.97	9.70	31.03	0.25	0.15	0.03	0.07
ZJ-9	1.92	9.40	31.32	0.18	0.12	0.01	0.05
Ave (ZJ)	1.98	8.38	33.72	0.25	0.16	0.03	0.06
XJ-1	2.05	9.73	33.43	1.70	1.21	0.05	0.44
XJ-2	1.76	5.25	34.61	1.05	0.67	0.03	0.35
XJ-3	1.94	12.28	31.8	2.45	0.64	0.09	1.72
XJ-4	1.64	14.34	27.38	2.40	0.77	0.13	1.50
XJ-5	1.97	11.67	29.58	0.37	0.19	0.02	0.16
XJ-6	1.63	7.55	28.16	0.41	0.27	0.05	0.09
XJ-7	1.57	6.66	30.77	0.33	0.22	0.03	0.08
XJ-8	1.86	8.08	32.02	0.37	0.24	0.04	0.09
XJ-9	1.36	14.69	25.66	0.31	0.21	0.03	0.07
XJ-10	2.04	9.01	24.89	0.34	0.28	0.04	0.02
XJ-11	1.90	13.96	30.02	0.30	0.23	0.03	0.04
XJ-12	1.80	7.70	30.93	0.39	0.29	0.06	0.04
XJ-13	1.99	6.26	30.30	0.42	0.31	0.07	0.04
XJ-14	1.63	7.83	28.52	0.29	0.18	0.02	0.09
XJ-15	1.77	4.83	30.17	0.20	0.13	0.01	0.07
XJ-16	2.16	7.91	26.56	0.18	0.06	0.01	0.11
XJ-17	1.74	7.04	28.5	0.22	0.14	0.01	0.07
Ave(XJ)	1.81	9.11	29.61	0.69	0.36	0.04	0.29

M, moisture; A_d , ash yield; V, volatile matter; S_t , total sulfur; S_p , pyritic sulfur; S_s , sulfate sulfur; S_o , organic sulfur.

The moisture (M) content of coal in Xinjier Mine is 1.26~2.16%, with an average of 1.81%. The ash yields (A_d) of coals in Xinjier Mine is 4.83~14.69%, with an average of 9.11%. The content of volatile matter (V) in Xinjier Mine coal is 24.89~34.61%, with an average of 29.61%. The total sulfur (S_t) content is 0.18~2.45%, with an average of 0.69%, and the pyritic sulfur (S_p), sulfate sulfur (S_s), and organic sulfur (S_o) accounts for 52.17%, 5.80%, and 42.03% of total sulfur, respectively. Among them, the total sulfur content in the XJ-1–XJ-4 areas are higher (Table 2). The coal samples from both mines could be classified as ultra-low moisture, low ash yield, medium-high volatile, and low-sulfur according to Chinese National Standards MT/850-2000 and GB/T 1522.4-2010.

4.2. Mineralogical Compositions

According to the XRD analyses results (Figure 3), the identified minerals in the Shanxi Formation raw coal samples are mainly kaolinite ($Al_4[Si_4O_{10}](OH)_8$), calcite ($CaCO_3$), quartz (SiO_2), and a small amount of pyrite (FeS_2). The microscopic morphology of pyrite is the aggregation of spherical, nodular, granular, framboidal, and fine-grained pyrite (Figure 4b,c). Banded (Figure 4d) and cell-filled kaolinite (Figure 4e) closely co-existed with pyrite (Figure 4f), formed at the same time as pyrite, and belong to the syngenetic minerals in the early diagenetic stage. Calcite is distributed in veins (Figure 4g) or filled with organic cell cavities (Figure 4h), which indicates epigenetic origin. Quartz is identified as filling the cell cavities of kinetoplastids (Figure 4i), indicating precipitation during peatification or early diagenetic stages.

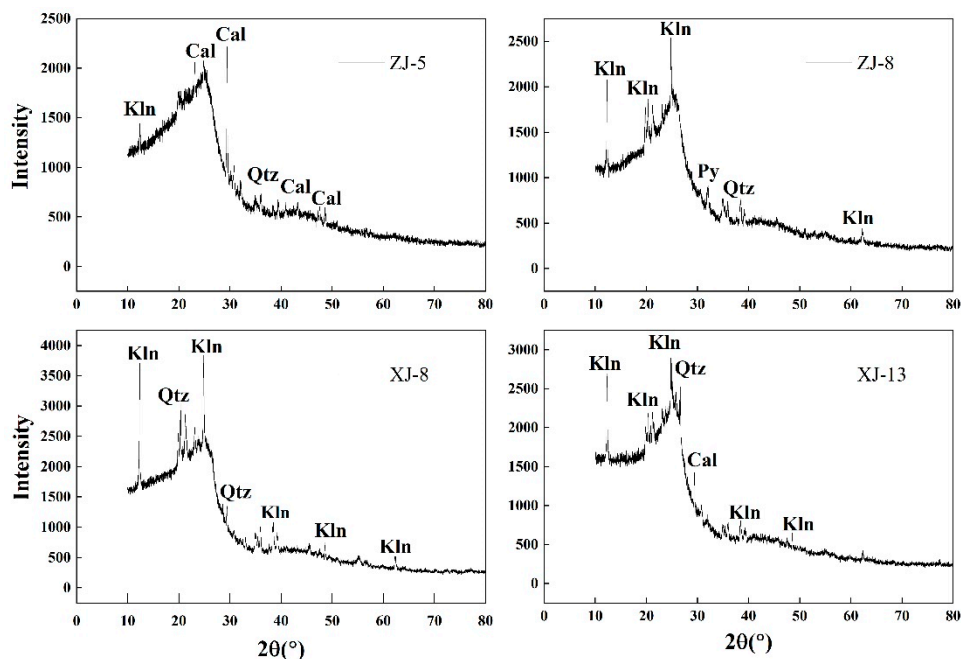


Figure 3. XRD analysis of the coal in the Shanxi Formation of Huainan (Kln—kaolinite; Qtz—quartz; Cal—calcite; Py—pyrite).

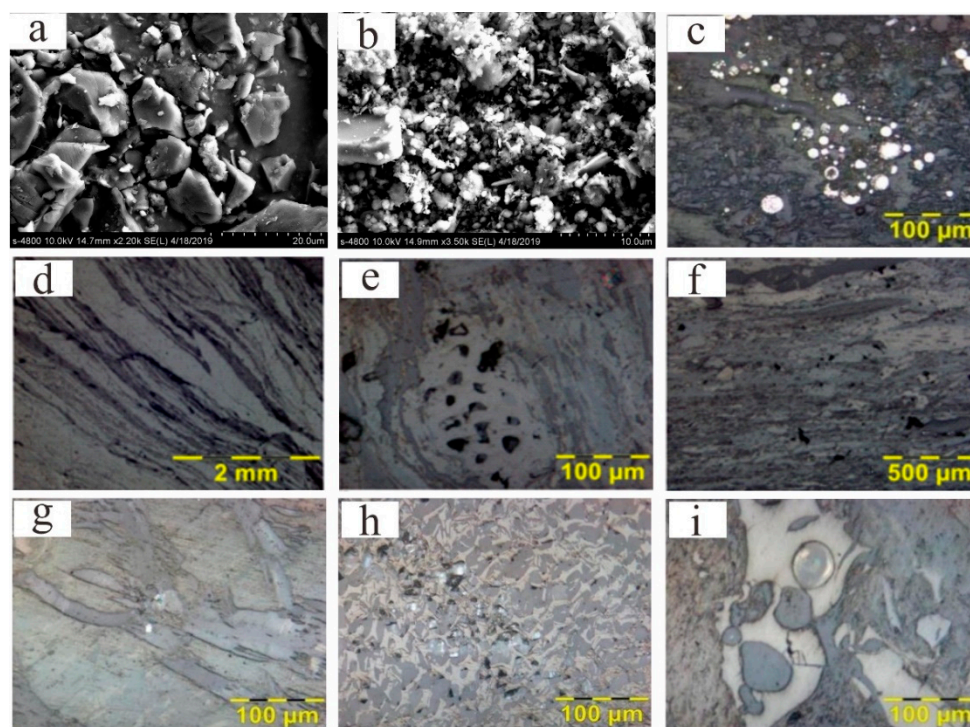


Figure 4. SEM (a,b) and optical images (c–i) of coal in Shanxi Formation. (Kln—kaolinite; Qtz—quartz; Py—pyrite) ((a,b): SEM image; (c): spherulitic pyrite; (d): banded kaolinite; (e): kaolinite filling the cell cavity; (f): co-existed with pyrite; (g): veined calcite; (h): calcite filling the cell cavity; (i): quartz filling the cell cavity).

4.3. Major Oxides

The average of major oxides of coal in the Zhangji mine is $\text{Al}_2\text{O}_3 > \text{SiO}_2 > \text{Fe}_2\text{O}_3 > \text{CaO} > \text{MgO} > \text{TiO}_2 > \text{Na}_2\text{O} > \text{P}_2\text{O}_5$, and the content ranges are Al_2O_3 (%) 1.81~6.21 (3.65), SiO_2 (%) 0.31~5.5 (2.89), Fe_2O_3 (%) 1.01~3.22 (1.68), CaO (%) 0.01~0.88 (0.35), MgO (%) 0.03~0.86 (0.24), TiO_2 (%) 0.05~0.51 (0.22), Na_2O (%) 0.05~0.06 (0.05), P_2O_5 (%) 0.01~0.08 (0.03). The $[w(\text{CaO}) + w(\text{MgO}) + w(\text{Fe}_2\text{O}_3)]/[w(\text{SiO}_2) + w(\text{Al}_2\text{O}_3)]$ ratio (C) of coal in the Zhangji mine ranges from 0.14~0.87 (0.41). The average of major oxides of coal in the Xinjier mine is $\text{SiO}_2 > \text{Al}_2\text{O}_3 > \text{CaO} > \text{Fe}_2\text{O}_3 > \text{MgO} > \text{TiO}_2 > \text{P}_2\text{O}_5 > \text{Na}_2\text{O}$, and the content ranges are SiO_2 (%) 2.13~24.13 (2.89), Al_2O_3 (%) 1.48~10.65 (3.65), CaO (%) 0.58~4.98 (0.35), Fe_2O_3 (%) 0.4~1.71 (1.68), MgO (%) 0.03~1.26 (0.24), TiO_2 (%) 0.11~0.48 (0.22), P_2O_5 (%) 0.02~0.17 (0.03), Na_2O (%) 0.01~0.11 (0.05). The C of coal in the Xinjier mine ranges from 0.19~0.41 (0.28) (Table 3). The main element oxides in Shanxi Formation coal are SiO_2 and Al_2O_3 , and the ash yield belongs to $\text{SiO}_2\text{-Al}_2\text{O}_3\text{-Fe}_2\text{O}_3\text{-CaO}$.

Table 3. Content range of major oxides in the coal of Shanxi Formation in Huainan (%).

Sample	Project	Al_2O_3	SiO_2	CaO	Fe_2O_3	MgO	P_2O_5	Na_2O	TiO_2	C	$\text{Al}_2\text{O}_3/\text{TiO}_2$
Zhangji Mine	Min	1.81	0.31	0.01	1.01	0.03	0.01	0.05	0.05	0.14	7.89
	Max	6.21	5.5	0.88	3.22	0.86	0.08	0.06	0.51	0.87	72.25
	Ave	3.65	2.89	0.35	1.68	0.24	0.03	0.05	0.22	0.41	27.67
Xinjier Mine	Min	1.48	2.13	0.58	0.4	0.03	0.02	0.01	0.11	0.19	13.45
	Max	10.65	24.13	4.98	1.71	1.26	0.17	0.11	0.48	0.41	35.63
	Ave	4.22	6.19	1.41	0.99	0.24	0.06	0.04	0.21	0.28	20.71

$$C = [w(\text{CaO}) + w(\text{MgO}) + w(\text{Fe}_2\text{O}_3)]/[w(\text{SiO}_2) + w(\text{Al}_2\text{O}_3)].$$

4.4. Content and Vertical Distribution of As

The As content in the Zhangji mine ranges from 12.51~95.03 mg/kg, with an average of 46.64 mg/kg, and the enrichment coefficient of As in Zhangji coal [21,22] (CC = content of trace elements/world average of elements in coal) is 5.62. The As content in the Xinjier mine ranges from 10.33~76.10 mg/kg, with an average of 43.73 mg/kg (Table 4), and the CC of As in Xinjier coal is 5.27. According to the Chinese coal industry standard (MT/T803-1999), the Shanxi Formation coal of Huainan Coalfield belongs to high As coal. In order to better understand the enrichment of As in coal, the As content in the coal of the Zhangji mine and Xinjier mine was compared with the Upper Shihezi and Lower Shihezi formation. The As of the Upper Shihezi formation is 6.27 mg/kg, while As in the Lower Shihezi formation is 4.81 mg/kg (Table 4). It can be seen that As shows obvious changes in the three mines. The As content in Shanxi formation coal was significantly higher than that in the Upper Shihezi and Lower Shihezi formations. However, there was a small difference in As content between the Upper Shihezi and the Lower Shihezi formations.

Table 4. Content of arsenic in coal from the Shanxi Formation in Huainan (mg/kg).

Sample	As	Sample	As
ZJ-1	42.73	XJ-1	29.14
ZJ-2	95.03	XJ-2	55.84
ZJ-3	23.54	XJ-3	12.08
ZJ-4	41.25	XJ-4	10.33
ZJ-5	13.38	XJ-5	69.16
ZJ-6	12.51	XJ-6	28.45
ZJ-7	73.96	XJ-7	41.01
ZJ-8	61.54	XJ-8	58.69
ZJ-9	55.78	XJ-9	63.05
Ave	46.64	XJ-10	42.52
XJ-T	244.65	XJ-11	48.95
XJ-P	107.97	XJ-12	76.10
XJ-B	124.65	XJ-13	57.92
Upper Shihezi ^a	6.27	XJ-14	11.13
Lower Shihezi ^a	4.81	XJ-15	33.76
Northern China ^b	3.92	XJ-16	67.60
World ^c	8.30	XJ-17	37.71
China ^d	3.79	Ave	43.73
USA ^e	24.00	-	-

^a From Chen et al. [14]. ^b From Tian et al. [8]. ^c From Ketris and Yudovich [21]. ^d From Dai et al. [22]. ^e From Finkelman et al. [23].

The vertical distribution characteristics of As content in coal are shown in Figure 5. The content of As changed significantly, among which XJ-4 (10.33 mg/kg) had the lowest content and ZJ-2 (95.03 mg/kg) had the highest content. The As content in the roof (XJ-T), parting (XJ-P), and floor (XJ-B) of the Shanxi formation is relatively high, and respectively are 244.65 mg/kg, 107.97 mg/kg, and 124.65 mg/kg (Table 4).

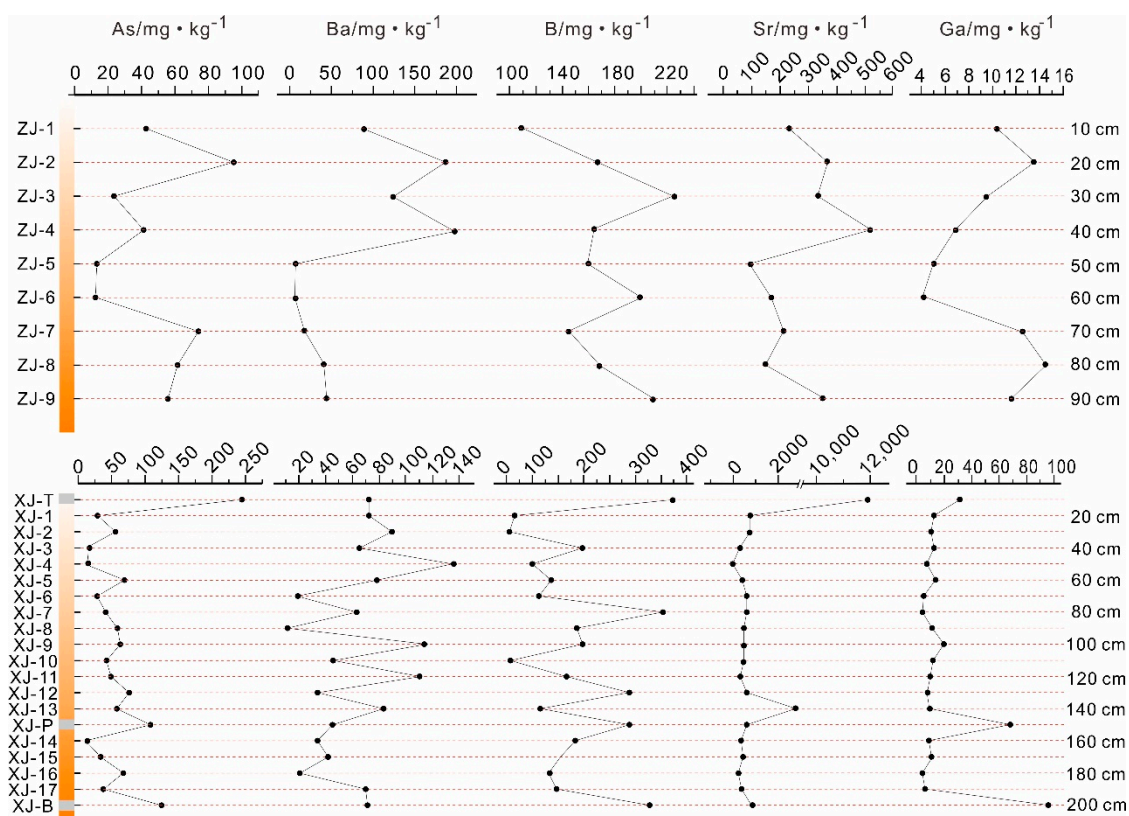


Figure 5. Vertical distribution of As, Ba, B, Sr, Ga in coal.

5. Discussion

5.1. Depositional Environment of Coal

The presence of high sulfur content is attributed to regional volcanism, peat environments, and depositional environments with strong sulfide mineralization [24,25]. Shanxi Formation coal is low-sulfur coal, but the total sulfur content in the XJ-1–XJ-4 area is relatively high (Table 2). Nevertheless, some previous studies show that the depositional environment affected by seawater may lead to the phenomenon of high sulfur in local coal seams [26]. The ash yield belongs to $\text{SiO}_2\text{-Al}_2\text{O}_3\text{-Fe}_2\text{O}_3\text{-CaO}$, indicating that more detritus minerals were transported to the study area and deposited on the coastal delta plain where it was open to clastic influx. The high content of SiO_2 and Al_2O_3 indicates that the minerals in the raw coal are composed of clay minerals (such as kaolinite and illite) and quartz [27]. In this study, the average ash yield of coal seams in the Shanxi Formation were considerably lower than coals from the Upper Shihezi Formation (20.12%) and Lower Shihezi Formation (21.27%) [28]. The change in ash content in the Huainan Coalfield is called “increasing stratigraphically upward” [14,29].

The $[w(\text{CaO}) + w(\text{MgO}) + w(\text{Fe}_2\text{O}_3)]/[w(\text{SiO}_2) + w(\text{Al}_2\text{O}_3)]$ ratio (C) of coal can indicate the depositional environment of the peat accumulation stage. Coal with $C \leq 0.22$ could be accumulated within terrestrial environments (e.g., freshwater lake-shore), whereas $C > 0.22$ could imply transition areas between terrestrial to shallow marine (e.g., back-mangrove conditions or delta front) [30,31]. The C in the coal of the Zhangji and Xinjier Mines is 0.41 and 0.28, respectively (Table 3), indicating that the sedimentary facies present sea-land alternate facies, where marine influence into paleomires could be common. However, in practice, the conclusion of C is often affected by other sedimentary environment indicators. For instance, the presence of gastropods, ostracod fauna, and charophyta remains obtained from coal seams in northern Turkey points to the predominance of freshwater conditions. Peat is deposited in sloughs with water from karst aquifers rich in sulfate and calcium; in this case, freshwater coal exhibits characteristics similar to saltwater or ocean-influenced peat/coal [32]. Furthermore, the presence of clastic Mg-bearing silicates or clay minerals

(e.g., chlorite or smectite) inputs into freshwater lakes, which increases the supply of dissolved Mg ions; in turn, the C values could be elevated [33]. Therefore, paleontological study of Shanxi Formation coal seams should be undertaken in the future for better understanding of the marine influence on peat-forming environments. Previous studies have suggested that $\text{Al}_2\text{O}_3/\text{TiO}_2$ is the most effective indicator for the properties of sedimentary parent rock. When the ratio of $\text{Al}_2\text{O}_3/\text{TiO}_2$ is 3:8, 8:21, or 21:70, it means that the sediments are formed by mafic, intermediate, or felsic igneous rocks, respectively [34,35]. The values of $\text{Al}_2\text{O}_3/\text{TiO}_2$ in the Huainan Shanxi Formation were widely distributed, ranging from 7.89 to 72.25, with an average of 24.19, indicating that the clastic materials in the coal mainly come from felsic rocks [36].

Even though B enrichments could be controlled by several parameters, the mass fraction of B has a good linear relationship with the paleo-salinity [23,26,37–39]. Generally, 50 mg/kg and 110 mg/kg are divided into fresh water/mildly brackish water and mildly brackish water/brackish water [40]. The highest content of B in Shanxi Formation coal is 354.60 mg/kg, with an average of 162.00 mg/kg (Table 5). Among them, the content range of B in the five coal samples of ZJ-1, XJ-1, XJ-2, XJ-4, and XJ-10 is between 50 mg/kg and 110 mg/kg, and other samples are all more than 110 mg/kg. This showed that Huainan Shanxi Formation is in the stage of mildly brackish-brackish water deposition (Figure 6a). In addition, the $w(\text{Sr})/w(\text{Ba})$ is a geochemical indicator that distinguishes between terrestrial and marine sedimentary environments in terrigenous clastic sediments [41]. $w(\text{Sr})/w(\text{Ba}) < 0.6$ indicated terrestrial freshwater deposition, $w(\text{Sr})/w(\text{Ba})$ between 0.6–1 suggested mildly brackish water deposition, and $w(\text{Sr})/w(\text{Ba}) > 1$ indicated brackish water deposition [41,42]. The $w(\text{Sr})/w(\text{Ba})$ ratio of the 26 samples in the Huainan Shanxi Formation was greater than 1 (Figure 6b), suggesting that the depositional environment of the Shanxi Formation was brackish water deposition. However, the usability of this indicator ($w(\text{Sr})/w(\text{Ba})$) is not widely acknowledged. Therefore, to verify this theory and accurately determine the differences between the sedimentary geochemical behaviors of Sr and Ba under different salinity conditions, it is recommended that in future studies, selective extraction of the Sr and Ba concentrations of different salinities is used to discriminate between marine and terrestrial sedimentary environments in terrigenous clastic sediments. An alternative geochemical indicator of the depositional environments is $w(\text{B})/w(\text{Ga})$ ratio in coals, that is, fresh water (<3), brackish water influences (3–5) and brackish water influences (>5) [43]. The values of $w(\text{B})/w(\text{Ga})$ in XJ-2 and XJ-10 in Shanxi Formation coal in the study area are slightly lower than the mildly brackish water/brackish water boundary value of 5, and other samples $w(\text{B})/w(\text{Ga})$ are greater than 5 (Figure 6c). In conclusion, the depositional environment of Shanxi Formation in Huainan is mildly brackish-brackish water deposition.

Table 5. The content range of B, Sr, Ba and Ga in coal.

Project	B (mg/kg)	Sr (mg/kg)	Ba (mg/kg)	Ga (mg/kg)	Sr/Ba	B/Ga
Min	52.32	71.29	11.74	4.22	1.65	4.81
Max	354.6	2742.71	135.69	20.37	17.72	48.44
Ave	162	585.08	72.35	9.87	5.81	20.57

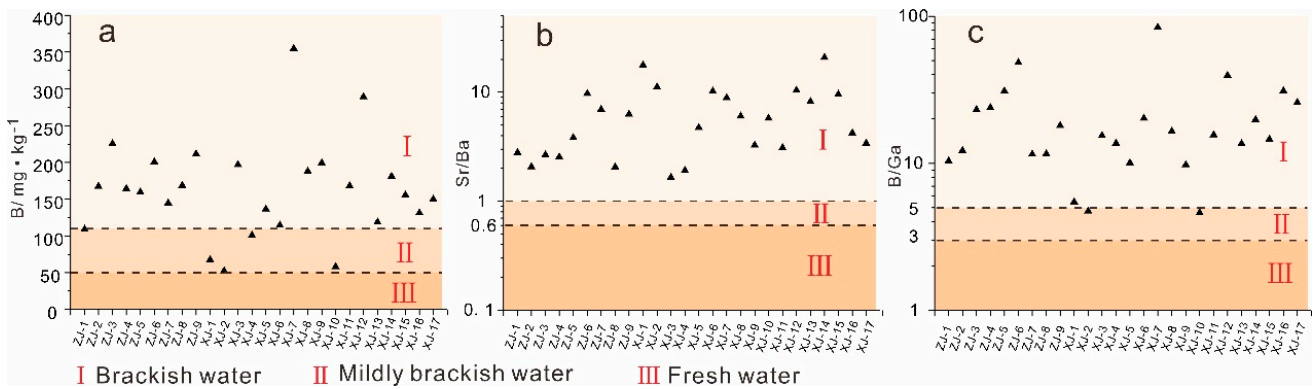


Figure 6. Judging the depositional environment of the Huainan Shanxi Formation. (a): B; (b): $w(\text{Sr})/w(\text{Ba})$; (c): $w(\text{B})/w(\text{Ga})$.

5.2. Geochemistry of As

The occurrence of As in coal is complicated, and it participates in the formation of inorganic or organic bound states in the structure of coal. For coal samples with a narrow ash yield range, correlation coefficients can help to infer how trace elements are present in coal in depositional environments [44]. In this study, we analyzed the correlation between As and ash, sulfur, and coal ash components, and combined with sequential chemical extraction experiment to explore the occurrence of As in the coals of Shanxi formation. Generally, As has a strong affinity for sulfur, and the relationship between As and sulfur increases and decreases simultaneously [45]. In this study, As and S contents are negatively correlated ($r = -0.41$), suggesting that less sulfur-arsenic minerals were present in the studied coal samples. However, the lack of As in SEM-EDX spectra does not mean that either pyrite or clay minerals do not contain As. Since the As measurement capacity is low, measurable amounts of As could not be seen in SEM-EDX spectra. Of course, the lack of As within framboidal pyrite grains are expectable, since these grains could have lower As concentrations [6,46]. On the other hand, the correlation coefficient between As and ash content was 0.53, showing a positive correlation (Figure 7a), indicating that the main carrier of As in coal might be affiliated with aluminosilicate minerals in the studied samples (e.g., clay minerals). In agreement with this correlation, As is positively correlated with Al_2O_3 and TiO_2 , indicating that As could be mainly affiliated with clay minerals in coal samples [47,48]. According to the result of sequential chemical extraction experiment (Figure 7b), the order of As content in each speciation is residual > Fe-Mn oxides > organic > exchangeable > carbonate. The main speciation of As is residual with 81.36%. The residual is difficult to dissolve by weak acid and general solvent, and its chemical activity is weak in the environment.

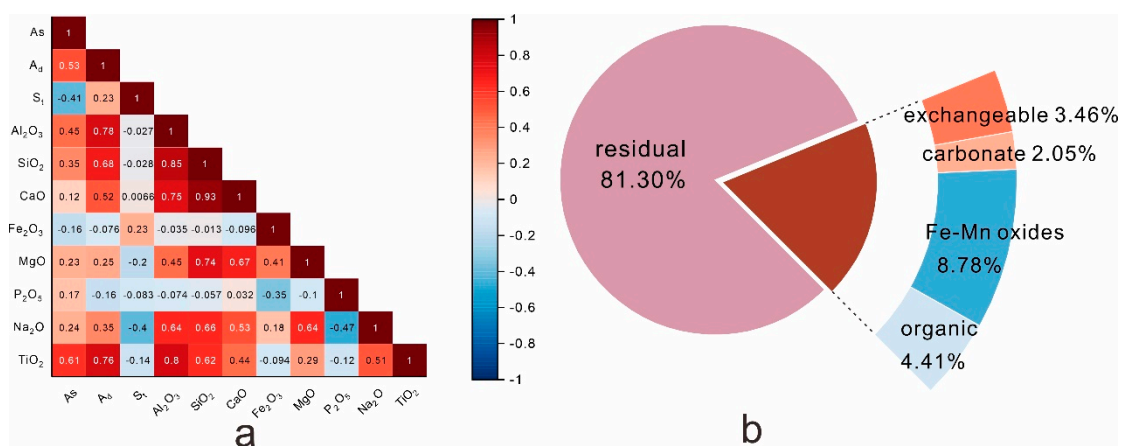


Figure 7. Correlation analysis (a) and speciation distribution of As (b) in coal.

The As distribution in the study area varies widely, which is mainly related to the peat-forming environment and mineralogical compositions of coal seams. This study shows that the Shanxi formation was deposited in a brackish environment, with decreasing marine influence along stratigraphy upward, increasing input of terrigenous detrital materials and significantly reduced content of As. Influenced by the depositional environment of Shanxi formation, there are clastic influxes of different origins in the roof (XJ-T), parting (XJ-P), and floor (XJ-B), which causes Shanxi Formation coal to have a special rock roof and good waterproof roof, parting and floor. The roof is a thick sandstone mainly composed of feldspar, and the floor is made up of aquifer-bearing Carboniferous, Ordovician, and Cambrian formations. The parting is mostly mudstone or carbonaceous mudstone, which will lead to high trace elements in the roof, parting, and floor. In the early and end stages of peat mires, the higher concentration of mineral solution seems to penetrate into paleomires, and the change of environmental conditions is not conducive to the normal growth of plants; trace elements are precipitated due to the obstructed circulation process, which leads to the higher content of trace elements in the top and bottom layers [49]. Due to the influence of depositional environment, a thin layer of mudstone and carbonaceous mudstone with high trace elements in gangue inclusion is formed.

5.3. Controlling Factors on As Enrichment

There are generally one or more particular geological factors that may influence the enrichment of trace elements in coals for different coal basins and coal forming periods [50,51]. The As content in Shanxi Formation coal in the Huainan Coalfield is obviously higher than that of the Upper Shihezi and Lower Shihezi formations, which indicates that As may have local enrichment characteristics and is closely related to the depositional environment of coal seam.

The contents of B and As in the Huainan Permian Upper Shihezi Formation (No. 11 and 13 coal seams), Lower Shihezi Formation (No. 4, 5, 6, 7, 8, and 9 coal seams), and Shanxi Formation No. 1 coal seam are shown in Figure 8 [14]. The high B contents in the No. 1 coal seam indicates that the peat marsh formed in the Shanxi Formation was greatly affected by sea water. Boron content in each coal seam of the Shihezi Formation indicates that the upper and lower Shihezi Formation are generally transitional phase or brackish water deposition environments, and the B content in No. 5 coal seam and No. 11 coal seam is lower than the fresh water/mildly brackish water boundary value 50 mg/kg, which is characterized by continental deposition.

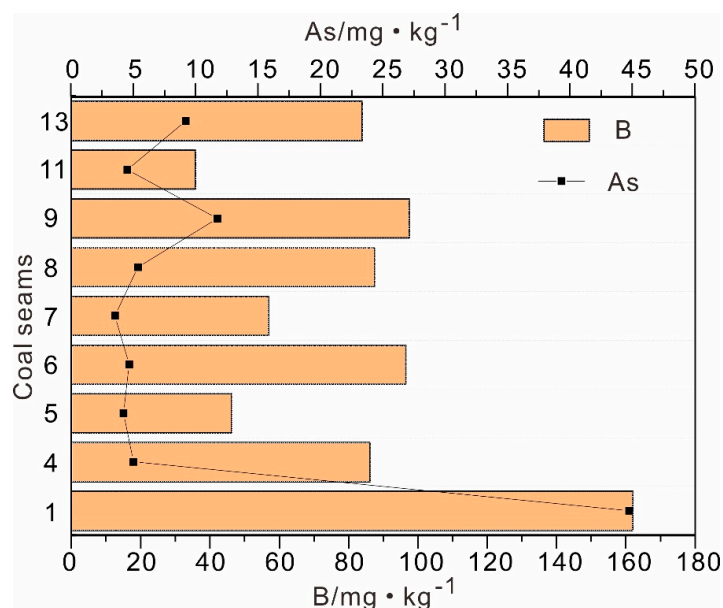


Figure 8. Content changes of B and As in different coal seams in Huainan.

During the Permian, several transgressions and regressions took place in the study area. The change trend of B contents in the longitudinal direction of the No. 1 coal seam in the Shanxi Formation to the No. 4–9 coal seams in the Lower Shihezi Formation to the No. 11 and 13 coal seams in the Upper Shihezi Formation is the same as that of As. The No. 1 coal seam of the Shanxi Formation was more affected by seawater than the coal seams of the Shihezi Formation. The S content in the coal has the overall order of Shanxi Formation > Lower Shihezi Formation > Upper Shihezi Formation. In this study, As occurs less in sulfides and more in silico-aluminate minerals. This shows that As in Shanxi Formation coal is mainly derived from terrestrial detrital sediments, which were brought into coal-forming mires by water and adsorbed into coal by humic acid, leading to enrichment of As in coal. Appropriate depositional environments can lead to relatively enriched As in coal.

6. Conclusions

The coal in the Shanxi Formation belongs to the ultra-low ash, ultra-low total moisture, medium-high volatile, low-sulfur coal category. The major minerals include quartz, kaolinite, calcite, and a small amount of pyrite. The coal in the Huainan Shanxi Formation was mainly affected by seawater, and the detrital material in the coal mainly comes from felsic rock. The enrichment coefficient CC of the coal is 5.39, which is characterized by enrichment. Among the samples, there are clastic materials from different sources in the roof, floor, and parting, and the As content is significantly higher than that in the coal. The residual state is the main form of As, and As is mainly found in clay minerals such as aluminosilicate. In addition, the recognition results of paleo-salinity characteristics indicate that the environment as a whole is brackish-saltwater sedimentation. A suitable depositional environment can lead to the relative enrichment of As in coal. The main source of As is terrigenous detritus, which is carried into the coal-marsh by water and adsorbed into coal by humic acid, thus leading to the enrichment of As in coal.

Author Contributions: Writing—original draft, L.Z. (Liqun Zhang); Writing—review and editing, L.Z. (Liqun Zhang); Methodology, L.Z. (Liqun Zhang) and M.L.; Investigation, L.Z. (Liqun Zhang); Software, L.Z. (Liqun Zhang); Conceptualization, L.Z. (Liugen Zheng); Resources, L.Z. (Liugen Zheng); Funding acquisition, L.Z. (Liugen Zheng); Supervision, L.Z. (Liugen Zheng); Data curation, M.L. All authors have read and agreed to the published version of the manuscript.

Funding: This research was supported by the University Synergy Innovation Program of Anhui Province (GXXT-2021-017) and the National Natural Science Foundation of China (42072201). We acknowledge the editors and reviewers for polishing the language and for in-depth discussion.

Institutional Review Board Statement: Not applicable.

Informed Consent Statement: Not applicable.

Data Availability Statement: All data generated or used during the study appear in the submitted article.

Conflicts of Interest: The authors declare no conflict of interest.

References

1. Kang, Y.; Liu, G.J.; Chou, C.L.; Wong, M.H.; Zheng, L.G.; Ding, R. Arsenic in Chinese coals: Distribution, modes of occurrence, and environmental effects. *Sci. Total Environ.* **2011**, *412*–*413*, 1–13. [[CrossRef](#)]
2. Hu, G.Q.; Liu, G.J.; Wu, D.; Fu, B. Geochemical behavior of hazardous volatile elements in coals with different geological origin during combustion. *Fuel* **2018**, *233*, 361–376. [[CrossRef](#)]
3. Zhang, L.Q.; Zhou, H.H.; Chen, X.; Liu, G.J.; Jiang, C.L.; Zheng, L.G. Study of the micromorphology and health risks of arsenic in copper smelting slag tailings for safe resource utilization. *Ecotoxicol. Environ. Saf.* **2021**, *219*, 112321. [[CrossRef](#)] [[PubMed](#)]
4. Dai, S.F.; Zeng, R.S.; Sun, Y. Enrichment of arsenic, antimony, mercury, and thallium in a Late Permian anthracite from Xingren, Guizhou, Southwest China. *Int. J. Coal Geol.* **2006**, *66*, 217–226. [[CrossRef](#)]
5. Diehl, S.F.; Goldhaber, M.B.; Koenig, A.E.; Lowers, H.A.; Ruppert, L.F. Distribution of arsenic, selenium, and other trace elements in high pyrite Appalachian coals: Evidence for multiple episodes of pyrite formation. *Int. J. Coal Geol.* **2012**, *94*, 238–249. [[CrossRef](#)]

6. Karayığit, A.; Bircan, C.; Mastalerz, M.; Oskay, R.; Querol, X.; Lieberman, N.; Türkmenb, I. Coal characteristics, elemental composition and modes of occurrence of some elements in the İsaalan coal (Balıkesir, NW Turkey). *Int. J. Coal Geol.* **2017**, *172*, 43–59. [[CrossRef](#)]
7. Yudovich, Y.E.; Ketris, M.P. Mercury in coal: A review: Part 1. Geochemistry. *Int. J. Coal Geol.* **2005**, *62*, 107–134. [[CrossRef](#)]
8. Tian, H.Z.; Zhu, C.Y.; Gao, J.J.; Cheng, K.; Hao, J.M.; Wang, K.; Hua, S.B.; Wang, Y.; Zhou, J.R. Quantitative assessment of atmospheric emissions of toxic heavy metals from anthropogenic sources in China: Historical trend, spatial distribution, uncertainties, and control policies. *Atmos. Chem. Phys.* **2015**, *15*, 10127–10147. [[CrossRef](#)]
9. Fu, C.; Bai, X.F.; Jiang, Y. Discussion on the relationship between the content of Arsenic and the coal quality characteristic and the Arsenic modes of occurrence in Chinese high Arsenic coal. *J. China Coal Soc.* **2012**, *37*, 96–102. (In Chinese)
10. Zhang, Y.Y.; Tian, J.J.; Feng, S.; Yang, F.; Lu, X.Y. The occurrence modes and geologic origins of arsenic in coal from Santanghu Coalfield, Xinjiang. *J. Geochem. Explor.* **2018**, *186*, 225–234. [[CrossRef](#)]
11. Li, B.; Zhuang, X.; Li, J.; Querol, X.; Font, O.; Moreno, N. Enrichment and distribution of elements in the Late Permian coals from the Zhina Coalfield, Guizhou Province, Southwest China. *J. Geochem. Explor.* **2017**, *171*, 111–129. [[CrossRef](#)]
12. Sun, R.Y.; Liu, G.J.; Zheng, L.G.; Chou, C.L. Characteristics of coal quality and their relationship with coal-forming environment: A case study from the Zhuji exploration area, Huainan coalfield, Anhui, China. *Energy* **2010**, *35*, 423–435. [[CrossRef](#)]
13. Sun, R.Y.; Liu, G.J.; Zheng, L.G.; Chou, C.L. Geochemistry of trace elements in coals from the Zhuji mine, Huainan coalfield, Anhui, China. *Int. J. Coal Geol.* **2010**, *81*, 81–96. [[CrossRef](#)]
14. Chen, J.; Liu, G.J.; Jiang, M.M.; Chou, C.L.; Li, H.; Wu, B.; Zheng, L.G.; Jiang, D.D. Geochemistry of environmentally sensitive trace elements in Permian coals from the Huainan coalfield, Anhui, China. *Int. J. Coal Geol.* **2011**, *88*, 41–54. [[CrossRef](#)]
15. Chen, S.; Wu, D.; Liu, G.; Sun, R.; Fan, X. Geochemistry of major and trace elements in Permian coal: With an emphasis on no. 8 coal seam of Zhuji coal mine, Huainan coalfield, China. *Environ. Earth Sci.* **2016**, *75*, 494. [[CrossRef](#)]
16. Dai, S.F.; Liu, J.J.; Ward, C.R.; Hower, J.C.; French, D.; Jia, S.H.; Hood, M.M.; Garrison, T.M. Mineralogical and geochemical compositions of Late Permian coals and host rocks from the Guxu Coalfield, Sichuan Province, China, with emphasis on enrichment of rare metals. *Int. J. Coal Geol.* **2016**, *166*, 71–95. [[CrossRef](#)]
17. Munir, M.A.M.; Liu, G.J.; Yousaf, B.; Ali, M.U.; Abbas, Q.; Ullah, H. Enrichment of Bi-Be-Mo-Cd-Pb-Nb-Ga, REEs and Y in the Permian coals of the Huainan Coalfield, Anhui, China. *Ore Geol. Rev.* **2018**, *95*, 431–455. [[CrossRef](#)]
18. Wang, G.; Ju, Y.; Yan, Z.; Li, Q. Pore structure characteristics of coal-bearing shale using fluid invasion methods: A case study in the Huainan–Huabei Coalfield in China. *Mar. Pet. Geol.* **2015**, *62*, 1–13. [[CrossRef](#)]
19. Chen, S.; Wu, D.; Liu, G.; Sun, R. Raman spectral characteristics of magmatic-contact metamorphic coals from Huainan Coalfield, China. *Spectrochim. Acta Part A Mol. Biomol. Spectrosc.* **2017**, *171*, 31–39. [[CrossRef](#)]
20. Wei, Q.; Hu, B.; Li, X.; Feng, S.; Xu, H.; Zheng, K.; Liu, H. Implications of geological conditions on gas content and geochemistry of deep coalbed methane reservoirs from the Panji Deep Area in the Huainan Coalfield, China. *J. Nat. Gas Sci. Eng.* **2021**, *85*, 103712. [[CrossRef](#)]
21. Ketris, M.P.; Yudovich, Y.E. Estimations of Clarkes for Carbonaceous biolithes: World averages for trace element contents in black shales and coals. *Int. J. Coal Geol.* **2009**, *78*, 135–148. [[CrossRef](#)]
22. Dai, S.F.; Luo, Y.B.; Seredin, V.V.; Ward, C.R.; Hower, J.C.; Zhao, L.; Liu, S.D.; Zhao, C.L.; Tian, H.M.; Zou, J.H. Revisiting the late Permian coal from the Huayingshan, Sichuan, southwestern China: Enrichment and occurrence modes of minerals and trace elements. *Int. J. Coal Geol.* **2014**, *122*, 110–128. [[CrossRef](#)]
23. Finkelman, R.; Dai, S.; French, D. The importance of minerals in coal as the hosts of chemical elements: A review. *Int. J. Coal Geol.* **2019**, *212*, 103251. [[CrossRef](#)]
24. Chou, C.L. Sulfur in coals: A review of geochemistry and origins. *Int. J. Coal Geol.* **2012**, *100*, 1–13. [[CrossRef](#)]
25. Dai, S.F.; Bechtel, A.; Eble, C.; Flores, R.; French, D.; Graham, I.T.; Hood, M.M.; Hower, J.C. Recognition of peat depositional environments in coal: A review. *Int. J. Coal Geol.* **2020**, *219*, 103383. [[CrossRef](#)]
26. Karayığit, A.I.; Atalay, M.; Oskay, R.G.; Córdoba, P.; Querol, X.; Bulut, Y. Variations in elemental and mineralogical compositions of Late Oligocene, Early and Middle Miocene coal seams in the Kale-Tavas Molasse sub-basin, SW Turkey. *Int. J. Coal Geol.* **2020**, *218*, 103366. [[CrossRef](#)]
27. Munir, M.A.M.; Liu, G.J.; Yousaf, B.; Ali, M.U.; Abbas, Q. Enrichment and distribution of trace elements in Padhrar, Thar and Kotli coals from Pakistan: Comparison to coals from China with an emphasis on the elements distribution. *J. Geochem. Explor.* **2018**, *185*, 153–169. [[CrossRef](#)]
28. Ding, D.S.; Liu, G.J.; Fu, B.; Qi, C.C. Characteristics of the coal quality and elemental geochemistry in Permian coals from the Xinjier mine in the Huainan Coalfield, north China: Influence of terrigenous inputs. *J. Geochem. Explor.* **2018**, *186*, 50–60.
29. Fu, B.; Liu, G.J.; Liu, Y.; Cheng, S.W.; Qi, C.C.; Sun, R.Y. Coal quality characterization and its relationship with geological process of the Early Permian Huainan coal deposits, southern North China. *J. Geochem. Explor.* **2016**, *166*, 33–44. [[CrossRef](#)]
30. Jiang, Y.F.; Zhao, L.; Zhou, G.Q.; Wang, X.B.; Zhao, L.X.; Wei, J.P.; Song, H.J. Petrological, mineralogical, and geochemical compositions of Early Jurassic coals in the Yining Coalfield, Xinjiang, China. *Int. J. Coal Geol.* **2015**, *152*, 47–67. [[CrossRef](#)]
31. Li, C.H.; Liang, H.D.; Wang, S.K.; Liu, G.J. Study of harmful trace elements and rare earth elements in the Permian tectonically deformed coals from Lugou Mine, North China Coal Basin, China. *J. Geochem. Explor.* **2018**, *190*, 10–25. [[CrossRef](#)]
32. Oskay, R.G.; Christanis, K.; Inaner, H.; Salman, M.; Taka, M. Palaeoenvironmental reconstruction of the eastern part of the Karapınar-Ayrancı coal deposit (Central Turkey). *J. Geochem. Explor.* **2016**, *163*, 100–111. [[CrossRef](#)]

33. Dill, H.G. A geological and mineralogical review of clay mineral deposits and phyllosilicate ore guides in Central Europe—A function of geodynamics and climate change. *Ore Geol. Rev.* **2020**, *119*, 103304. [[CrossRef](#)]
34. Dai, S.F.; Hower, J.C.; Ward, C.R.; Guo, W.M.; Song, H.J.; O’Keefe, J.M.K.; Xie, P.P.; Hood, M.M.; Yan, X.Y. Elements and phosphorus minerals in the middle Jurassic inertinite-rich coals of the Muli Coalfield on the Tibetan Plateau. *Int. J. Coal Geol.* **2015**, *144–145*, 23–47. [[CrossRef](#)]
35. He, B.; Xu, Y.G.; Zhong, Y.T.; Guan, J.P. The Guadalupian-Lopingian boundary mudstones at Chaotian (SW China) are clastic rocks rather than acidic tuffs: Implication for a temporal coincidence between the end-Guadalupian mass extinction and the Emeishan volcanism. *Lithos* **2010**, *119*, 10–19. [[CrossRef](#)]
36. Song, D.Y.; Li, C.H.; Song, B.Y.; Yang, C.B.; Li, Y.B. Geochemistry of mercury in the Permian tectonically deformed coals from Peigou mine, Xinmi coalfield, China. *Acta Geol. Sin.-Engl. Ed.* **2017**, *91*, 2243–2254. [[CrossRef](#)]
37. Beaton, A.P.; Goodarzi, F.; Potter, J. The petrography, mineralogy and geochemistry of a paleocene lignite from southern Saskatchewan, Canada. *Int. J. Coal Geol.* **1991**, *17*, 117–148. [[CrossRef](#)]
38. Chen, J.; Chen, P.; Yao, D.; Liu, Z.; Wu, Y.; Liu, W.; Hu, Y. Mineralogy and geochemistry of Late Permian coals from the Donglin Coal Mine in the Nantong coalfield in Chongqing, southwestern China. *Int. J. Coal Geol.* **2015**, *149*, 24–40. [[CrossRef](#)]
39. Dai, S.F.; Liu, J.; Ward, C.R.; Hower, J.C.; Xie, P.; Jiang, Y. Petrological, geochemical, and mineralogical compositions of the low-Ge coals from the Shengli Coalfield, China: A comparative study with Ge-rich coals and a formation model for coal-hosted Ge ore deposit. *Ore Geol. Rev.* **2015**, *71*, 318–349. [[CrossRef](#)]
40. Alastuey, A.; Jiménez, A.; Plana, F.; Querol, X.; Suárez-Ruiz, I. Geochemistry, mineralogy, and technological properties of the main Stephanian (Carboniferous) coal seams from the Puertollano Basin, Spain. *Int. J. Coal Geol.* **2001**, *45*, 247–265. [[CrossRef](#)]
41. Wang, A.; Wang, Z.; Liu, J.; Xu, N.; Li, H. The Sr/Ba ratio response to salinity in clastic sediments of the Yangtze River Delta. *Chem. Geol.* **2021**, *559*, 119923. [[CrossRef](#)]
42. Dai, S.; Hou, X.; Ren, D.; Tang, Y. Surface analysis of pyrite in the no. 9 coal seam, Wuda coalfield, Inner Mongolia, China, using high-resolution time-of-flight secondary ion mass-spectrometry. *Int. J. Coal Geol.* **2003**, *55*, 139–150. [[CrossRef](#)]
43. Hu, X.F.; Liu, Z.J.; Liu, R.; Liu, D.Q.; Zhang, M.M.; Xu, S.C.; Meng, Q.T. Trace Element Characteristics of Eocene Jijuntun Formation and the Favorable Metallogenic Conditions of Oil Shale in Fushun Basin. *J. Jilin Univ.* **2012**, *42*, 60–71.
44. Eskenazy, G.; Finkelman, R.B.; Chattarjee, S. Some considerations concerning the use of correlation coefficients and cluster analysis in interpreting coal geochemistry data. *Int. J. Coal Geol.* **2010**, *83*, 491–493. [[CrossRef](#)]
45. Xie, H.; Nie, A.G. The modes of occurrence and washing floatation characteristic of arsenic in coal from Western Guizhou. *J. China Coal Soc.* **2010**, *35*, 117–121.
46. Hower, J.C.; Campbell, J.L.; Teesdale, W.J.; Nejedly, Z.; Robertson, J.D. Scanning proton microprobe analysis of mercury and other trace elements in Fe-sulfides from a Kentucky coal. *Int. J. Coal Geol.* **2008**, *75*, 88–92. [[CrossRef](#)]
47. Sun, Y.Z.; Zhao, C.L.; Li, Y.H.; Wang, J.X.; Liu, S.M. Li distribution and mode of occurrences in Li-bearing coal seam # 6 from the Guanbanwusu Mine, Inner Mongolia, Northern China. *Energy Explor. Exploit.* **2012**, *30*, 109–130.
48. Wang, P.P.; Ji, D.P.; Yang, Y.C.; Zhao, L.X. Mineralogical compositions of Late Permian coals from the Yueliangtian mine, western Guizhou, China: Comparison to coals from eastern Yunnan, with an emphasis on the origin of the minerals. *Fuel* **2016**, *181*, 859–869. [[CrossRef](#)]
49. Liu, G.J.; Yang, P.Y.; Peng, Z.C.; Wang, G.L. Geochemistry of trace elements from the No.3 coal seam of Shanxi Formation in the Yanzhou mining district. *Geochimica* **2003**, *32*, 255–262.
50. Jiu, B.; Huang, W.; Mu, N. Mineralogy and elemental geochemistry of Permo-Carboniferous Li-enriched coal in the southern Ordos Basin, China: Implications for modes of occurrence, controlling factors and sources of Li in coal. *Ore Geol. Rev.* **2022**, *141*, 104686. [[CrossRef](#)]
51. Oboirien, B.O.; Thulari, V.; North, B.C. Enrichment of trace elements in bottom ash from coal oxy-combustion: Effect of coal types. *Appl. Energy* **2016**, *177*, 81–86. [[CrossRef](#)]